Waste and Biomass Valorization (2022) 13:2979–2989
https://doi.org/10.1007/s12649-022-01693-1

ORIGINAL PAPER

Effects of *Calamus*-Derived Biochar on the Thermophilic Anaerobic Digestion of Long-SRT Waste Activated Sludge from the Municipal Wastewater Treatment Plant

Yi Wang[1,2] · Zhi Wang[1,2] · Linping Wang[1,2] · Jun Peng[1,2] · Xiaomei Kou[3] · Lijuan Gao[3] · Shizhang Wu[3] · Baohua Chai[1,3] · Ke Zhao[1]

Received: 17 July 2021 / Accepted: 17 January 2022 / Published online: 15 February 2022

Abstract

In order to improve the efficiency of anaerobic digestion of long sludge retention time (SRT) sludge and seek a suitable disposal method for the massive plants harvested from constructed wetlands, we prepared *Calamus*-derived biochar (*Calamus*-BC) and added it to thermophilic anaerobic digestion (TAD) system of long SRT sludge. Moreover, the effect of *Calamus*-BC supplemental level (0, 5, 10, 15, 20 g/L) on TAD was explored through a series of batch experiments. Results showed that *Calamus*-BC addition can increase the conductivity and pH in TAD of long-SRT sludge obviously, thereby promoting methane production, reducing total VFAs accumulation and shortening the lag phases. When the *Calamus*-BC dosage was 15 g/L, the cumulative CH_4 yield reached the highest 246.73 mL/g VS, which was 43.4% higher than the control group. Furthermore, it proved the modified Gompertz model was suitable for the actual evolution of CH_4 production in TAD of long-SRT sludge. This study provided an alternative for efficient biomass stabilization and bioenergy recovery from long-SRT sludge and supplied a feasible resourceful approach for massive *Calamus* from constructed wetlands in water rehabilitation engineering.

Graphical Abstract

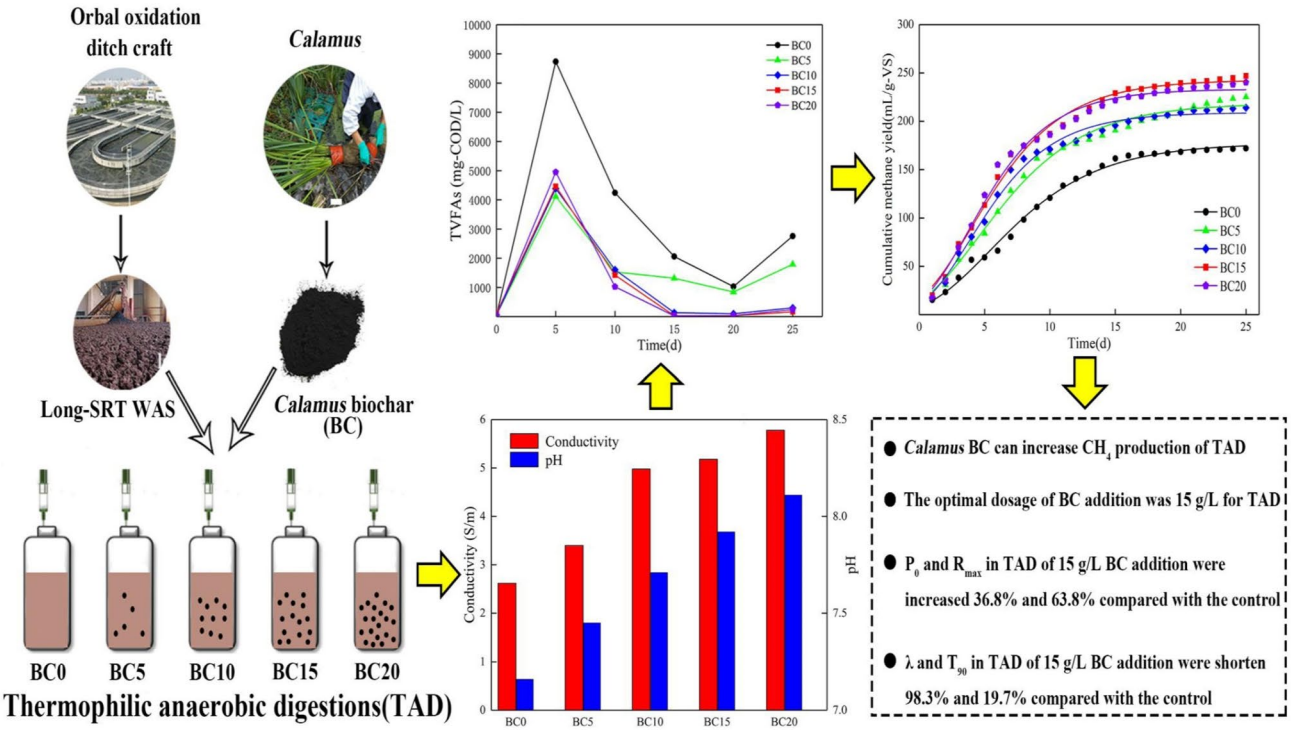

Extended author information available on the last page of the article

Keywords Thermophilic anaerobic digestion · Long-SRT sludge · *Calamus*-derived biochar · Methane production · Resource utilization

Statement of Novelty

This study is the first time to propose an economical and efficient additive that can improve the efficiency and stability in TAD of long-SRT sludge. The results could supply useful information for treating long-SRT sludge from BNR process and massive *Calamus* from constructed wetlands.

Introduction

Biological nutrient removal (BNR) processes are widely used in wastewater treatment plants to meet the stringent limits of N and P discharges in China. However, compared with the conventional waste sludge, the waste sludge from BNR is an organic matter that is difficult to degrade and usually has a long sludge retention time (SRT) and high contents of N and P due to the long generation cycle of nitrifying bacteria [1]. In addition, the increased amount of municipal wastewater often leads to a gradual increase in the output of waste sludge from wastewater treatment plants. In brief, the properties of the waste activated sludge (WAS) from the BNR process are significantly different from those produced from the traditional activated sludge process, and the waste sludge output of BNR increases with the urban sewage quantity. Therefore, it is necessary to find a suitable treatment method for the WAS produced from BNR process.

Anaerobic digestion (AD) has been applied as an important technology globally for sludge reduction, stabilization, and resource utilization [2–4], which can be operated at mesophilic (35 °C) and thermophilic (55 °C) temperatures on the basis of methanogenic bacteria requirements [5]. Although mesophilic AD (MAD) of WAS is applied widely because of its good stability, the biogas production effect of MAD is not ideal due to the complex structure, strong rigidity and slow dissolution and hydrolysis process of sludge flocs [6]. Therefore, to facilitate the disintegration of WAS, a lot of pretreatment technologies have been widely studied such as alkaline, thermal, ultrasonic, enzymatic and their combinations [7]. Considering the huge energy consumption and economic cost, pretreatment is not always suitable in sludge anaerobic digestion. Compared with MAD, thermophilic AD (TAD) has higher energy consumption and poorer stability, but it is considered to have a great application prospect because of its rapid hydrolysis rate, high gas production potential and high pathogen removal rate [8]. However, the research and the application on the TAD of WAS are lacking at present [9]. Therefore, it is necessary to study the stability of TAD of WAS to promote the practical application.

Acidification is one of the major factors for the poor stability of TAD [10]. The fermentation rates enhanced by TAD usually cause the accumulation of volatile fatty acids (VFAs), which further leads to digester failure through inhibiting the methanogenic activity due to decreased pH [11]. For instance, Shi et al. [12] have found a fivefold higher accumulation of total VFAs in the TAD compared with those in the MAD. On the other side, ammonia nitrogen is another major factor for TAD. Total ammonia nitrogen (TAN) exists as ammonium ions and free ammonia nitrogen (FAN), and FAN is the main toxic form, which can diffuse passively into microbial cells and cause proton imbalance [13]. FAN concentration is affected by pH, T, and equilibrium reactions as Eq. 1 [14].

$$\frac{FAN}{TAN} = \left\{ 1 + \frac{10^{-pH}}{10^{-\left[0.09018 + \frac{2729.92}{T(K)}\right]}} \right\}^{-1} \quad (1)$$

where T (K) refers to the Kelvin temperature. From the above formula, it is easy seen that higher pH would result in a higher concentration of FAN. In addition, the operation of digesters at elevated temperature would increases the negative effect of FAN. Therefore, the FAN concentration is another factor for the poor stability of the TAD [15, 16]. To resolve these problems, a variety of strategies that improve the stability of TAD are conducted, including domestication of resilient thermophilic microbiome, co-digestion with complementary substrates, microbial batteries, and application of conductive materials within TAD systems [17].

The direct interspecies electron transfer (DIET) is a recently discovered form of interspecies electron transfer, wherein the bacteria transfer electrons directly to methanogens without reliance on metabolites (e.g., H_2) [18]. The addition of conductive materials, such as active carbon, can enhance methanogenesis by promoting the DIET among bacteria and methanogens [19]. Moreover, active carbon can adsorb the inhibitory compounds during the anaerobic digestion process, which leads to the enhanced stability of anaerobic digestion [20]. It is well known that TAD is more unstable and easily accumulates the inhibitory compounds compared with MAD. However, most of the studies on the conductive materials addition are focused on the MAD, whereas very limited information is available on the effects of conductive material addition on TAD [21–23].

As an economical and efficient carbon material, biochar has been reported that can improve microbial activities and the system biostability in the AD process due

to the porous surface [24]. In addition, biochar was also proved to promote DIET by acting as an electronic conductor to metabolize ethanol during AD process [25]. Shen et al. [26] had observed that the biochar promoted the biostability of the AD process and enhanced the utilization of the digestion residues as soil amendment, which elevated the feasibility of biochar in AD processes. However, the effect of biochar made from waste *Calamus* in of constructed wetlands on sludge TAD is not clear. The constructed wetland is a cheap and widely applied facility in the rehabilitation of polluted water bodies, but it unavoidably produces a great deal of plants during water purification (such as *Calamus* and *Phragmites* communis etc.). These plants must be harvested to ensure the normal and stable operation of the constructed wetland when they are aged and withered regularly with the change of seasons. Thus, the produced plants cover a lot of land and increase the disposal costs of municipal solids [27]. Being the most popular plant in worldwide constructed wetlands, *Calamus* disposal becomes an important issue in the application of constructed wetlands.

This study aims to investigate the characterization of biochar derived from *Calamus* and explore the effects of *Calamus*-derived biochar (*Calamus*-BC) addition on the TAD of long-SRT sludge. Furthermore, the performance of the TAD reactor is evaluated in accordance with the production of CH_4, TAN, and VFAs at various concentrations of *Calamus*-BC. This study could supply an important strategy for the stable operation of long-SRT sludge TAD system and offer a low-cost alternative for the resource utilization of wetland plants.

Materials and Methods

Substrates and Inoculum

The dewatered activated sludge (DWAS) used in this study was collected from the sludge dewatering workshop of the third wastewater treatment plant of Xi'an, China, which adopted an orbal oxidation ditch craft to treat municipal wastewater of 200 000 m^3/day. The sludge is retented in the orbal oxidation ditch craft for 18–20 days, which led the waste sludge to be a typical long-SRT. The collected DWAS was stored at 4 °C before use, and its solid content was adjusted to 8% by using pure water when need to use as the substrate for this test. The inoculation sludge was collected from a laboratory-scale anaerobic reactor (35 °C) and domesticated for some time. The physicochemical properties of the DWAS and inoculation sludge are listed in Table 1.

Table 1 Physical and chemical properties of DWAS and inoculation sludge

Parameters	DWAS	Inoculation sludge
pH	7.2	7.01
TS (g/kg)	153.98	33.87
VS (g/kg)	91.60	16.58
VS/TS (%)	59.49	48.95
COD (g/kg)	115.56	96.69

Preparation and Characterization of *Calamus*-BC

The *Calamus* stem collected from a constructed wetland of Xi'an was heated at 105 °C for 24 h to completely remove H_2O, ground into a fine powder, and sieved using 100 mesh in this study. The biomass was filled in a porcelain crucible, compacted and covered tightly, then pyrolyzed in a muffle furnace at a heating rate of 20 °C/min to a final temperature of 600 °C for 2 h according to our optimum experiment previously. All biochar samples were stored in sealing bags before use.

The pH level of *Calamus*-BC was determined using a portable pH meter (PHS-3C) at a *Calamus*-BC to H_2O ratio of 1:20. The surface morphology of the *Calamus*-BC was observed using a scanning electron microscope (SEM, JSM-6510LV). The total surface area, pore size distribution, and pore volume of *Calamus*-BC were measured using the BET surface analyzer (V-Sorb 2800P).

TAD of WAS

Batch experiments were conducted in a series of serum bottles, including the total volume of 100 mL with the working volume of 60 mL, and the total volume of 250 mL with the working volume of 200 mL. The serum bottles of 100 mL were used for the biogas sample collection, and the serum bottles of 250 mL were used to collect the liquid samples for hydrolysis analysis. The inoculum–DWAS ratio used in the test was set to 20% (based on volatile solid). The series of experiments were set as BC0, BC5, BC10, BC15, and BC20 (setting three replicates), where BC0 represented the control group, and BC5, BC10, BC15, and BC20 represented the *Calamus*-BC concentrations of 5.0, 10.0, 15.0, and 20.0 g/L, respectively. All bottles were flushed with N_2 for 5 min to maintain anaerobic conditions and placed in a shaking water bath maintained at 52 °C and 140 r/min for TAD. Blank experiments with inoculum only were performed to remove the biogas produced from the inoculation sludge. The properties of each group of mixture at the beginning of the TAD are listed in Table 2.

Table 2 Parameters of each group of mixture at the beginning of TAD

Parameters	BC0	BC5	BC10	BC15	BC20
pH	7.16	7.45	7.71	7.92	8.11
TS (g/kg)	79.68	84.83	87.24	89.93	96.88
VS (g/kg)	44.65	47.82	49.31	52.06	54.93
VS/TS (%)	56.04	56.37	56.52	57.89	56.70
Conductivity (S/m)	2.62	3.40	4.98	5.18	5.78

Sample and Analytical Methods

The biogas production was determined daily by using a calibrated glass syringe. Biogas was collected once every five days, and its composition was analyzed by withdrawing a 300 μL sample using an Agilent syringe, then injecting it into a gas chromatograph (Agilent6890N, TCD) with a packed column (Agilent packed TDX-01). Argon was used as the carrier gas at a flow rate of 25 mL/min. The oven, column and detector temperature were 70, 100 and 170 °C, respectively. Liquid samples (10 mL) were collected from the serum bottle once every five days for determination. The pH was determined using a portable pH meter (PHS-3C). In addition, TS and VS were determined via the weight method. The TAN, soluble chemical oxygen demand (SCOD) and chemical oxygen demand (COD) were determined using standard methods (APHA, 1998). The samples were centrifuged at the relative centrifugal force of 8944 g for 10 min and passed through a cellulose acetate filter with pore size of 0.22 μm. The VFAs, including acetate, propionate, butyrate, and valerate, were analyzed using the GC (Agilent6890N, FID) equipped with a capillary column (PE WAX 30 m × 250 μm × 0.25 μm). Nitrogen was used as the carrier gas at a flow rate of 7.4 mL/min. The initial temperature for the oven, column and detector were 70, 220 and 300 °C and final temperature were 200, 220 and 300 °C, respectively.

Processing Parameters and Analysis

The modified Gompertz model (Eq. 2) was applied to determine the lag phase time (λ) and the maximum production potential (P_0). The time to produce 90% of CH_4 yield (T_{90}) and the time for effective CH_4 production (T_{ef}) [28] could be using Eqs. 3 and 4, respectively. Equation 1 was used to calculate the concentration of the FAN in accordance with the actual pH and temperature.

$$P = P_0 \cdot exp\left\{-exp\left[\frac{R_{max} \cdot e}{P_0}(\lambda - t)\right] + 1\right\} \quad (2)$$

$$T_{90} = \lambda + 3.25 \times \frac{P_0}{R_{max} \cdot e} \quad (3)$$

$$T_{ef} = T_{90} - \lambda \quad (4)$$

where P (L/kgVSadded) is the cumulative CH_4 yield at time t, e is exp (1) = 2.71828, R_{max} (L/kgVSadded/day) is the maximum specific CH_4 production rate, P_0 (L/kgVSadded) is the CH_4 production potential, and λ (day) is the lag phase time. The parameters in this equation (P_0, R_{max}, and λ) are estimated using the nonlinear fitting of Origin 2017.

Results and Discussion

Characterization of *Calamus*-BC

Figure 1 shows the SEM images of *Calamus*-BC, and Table S1 shows some parameters of *Calamus*-BC. Various micropores were connected to some narrow channels on the surface of *Calamus*-BC. The average pore size, total pore volume, and specific surface area (S_{BET}) of *Calamus*-BC were 153.9 nm, 0.68 cm^3/g, and 15.2 m^2/g, respectively. Xiong et al. [29] have reported that the biochar made from rice straw and rice husk have an S_{BET} of 61.681 and 41.512 m^2/g, respectively; total pore volume of 0.025 and 0.019 cm^3/g, respectively; and average pore size of 19.335 and 19.306 nm, respectively, under the same production conditions (pyrolysis at 600 °C for 2 h and sieving at 100 mesh). Thus, the *Calamus*-BC has smaller S_{BET} and a larger average pore size and total pore volume than the biochar made from rice straw and rice husk. Luo et al. [30] have reported that the physical characteristics of biochar especially porous structure can enhance the microbial activity and improve the resistance to various inhibitors by promoting the biofilm formation. At the same time, the porous structure promoted the methanation process due to acceleration of the DIET between bacteria and methanogens [31]. Therefore, the *Calamus*-BC could promote the CH_4 production process in TAD due to its porous structure.

Effects of Calamus-BC Dosage on the CH_4 Production in TAD

The batch experiment of 25 days was conducted. The daily biogas production rates of the test groups with *Calamus*-BC addition were evidently higher than that of the control group, and the biogas production rate increased with the increasing *Calamus*-BC dosage from day 1 to day 8 (Fig. S1). This finding might be ascribed to that the *Calamus*-BC increased the conductivity of the mixture (Table 2) and promoted the DIET process, thereby accelerating the biogas production

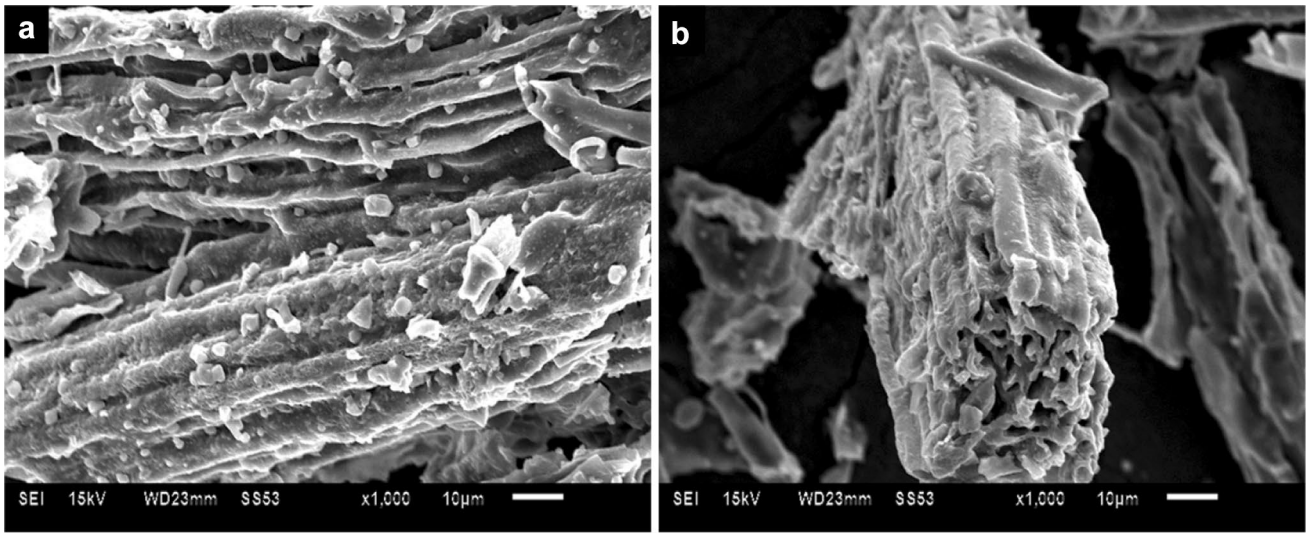

Fig. 1 Scanning electron microscope (SEM) of *Calamus*-BC: **a** tubular structure; **b** pore structure

rate. However, no significant difference was observed in the biogas production rate among the groups after eight days. The daily biogas production rate of BC15 was the highest among the four dosages and increased by 51.3% compared with the control group. Remarkably, the daily biogas production rate of the control group was higher than that of the test group on days 4, 8, and 11, which might be ascribed to that the test group had begun to decrease when the biogas production rate of the control group increased. These results indicated that the addition of *Calamus*-BC to TAD of long-SRT sludge led to an enhancement of CH_4 production rate but also caused the fluctuations of the CH_4 production in the initial stage of TAD.

The average contents of CH_4, CO_2, H_2, and N_2 in the total biogas volume during the whole experiment are shown in Table 3. The content of CH_4 in the biogas of BC5, BC10, and BC15 was 64%, whereas those of the BC0 and BC20 were 61% and 67%, respectively. The contents of CO_2 and N_2 in the biogas were 31–36% and 2–3%, respectively, but H_2 was not detected in all groups. Compared with that of the control group, the CH_4 content in the biogas of the BC20 group increased from 61 to 67%, and the CO_2 content decreased from 36 to 31%. There4fore, the addition of *Calamus*-BC increased the CH_4 content but reduced the CO_2 content, which might be attributed to the alkalinity of the biochar can convert CO_2 to HCO_3^- or CO_3^{2-}. This phenomenon increased the pH and promoted the CH_4 production [32].

Biochemical Methane Potential (BMP) Analysis

Based on the test results and the modified Gompertz model, the CH_4 production modeling was conducted (Fig. 2). The cumulative CH_4 production of the test group with the *Calamus*-BC addition was significantly higher than that of the control group (Table 3).

The kinetic parameters obtained using the nonlinear curve fit through the Gompertz model are listed in Table 4. The test group had significantly higher R_{max} ($mLCH_4$/ gVS/day) and P_0 ($mLCH_4$/gVS) than the control group. Compared with those in the control, R_{max} and P_0 were enhanced by 29.92% and 22.9%, respectively, in the BC5; 44.56% and 25.12%, respectively, in BC10; 63.91% and 36.83%, respectively, in BC15; and 76.08% and 61.48%, respectively, in BC20. The λ of the test groups was significantly lower than that of the control group. In addition, the T_{90} and the T_{ef} decreased with increasing *Calamus*-BC dosage, indicating

Table 3 Effects of the addition of biochar on gas production characteristics

Groups	Cumulative methane yield (mL/gVS)	Average CH_4 content (%)	Average CO_2 content (%)	Average N_2 content (%)
BC0	172.09	61	36	3
BC5	225.09	64	34	2
BC10	213.94	64	33	3
BC15	246.73	64	34	2
BC20	240.21	67	31	2

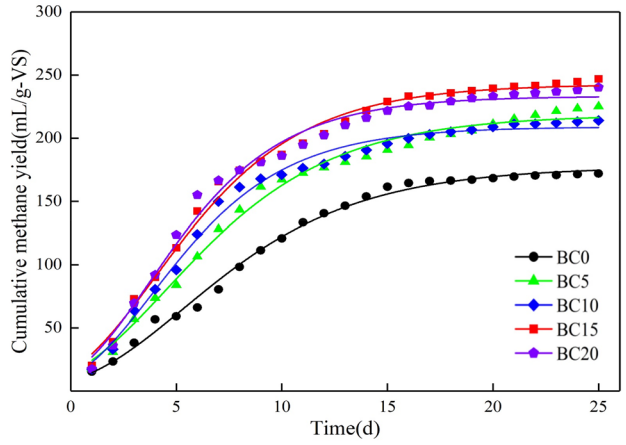

Fig. 2 Experimental data (symbols) and model simulation/prediction (lines) of cumulative methane yield

that the high *Calamus*-BC dosage shortened the retention time of sludge digestion efficiently.

Therefore, adding *Calamus*-BC to TAD system of the long-SRT sludge increased P_0 and R_{max} and effectively shortened λ of TAD. Shen et al. have reported that the addition of biochar enhances R_{max} and P_0 [33]. Jang et al. [34] have also found that λ in MAD and TAD of animal manure decreases by 26.9% and 24.4%, respectively, when 10 g/L biochar is added. This study showed that the proper addition of *Calamus*-BC (15 g/L) increased the CH_4 production. The excess addition of *Calamus*-BC might negatively affect the production of biogas and CH_4 in TAD.

Effects of *Calamus*-BC on the stability of TAD

The changes in SCOD and TVFAs concentration in the liquid phase during TAD are shown in Fig. 3. The changes in SCOD concentration in all groups increased rapidly at the beginning and then gradually decreased until the final increase after 20 days. On day 10, the differences in SCOD concentration of each group were evident, and a negative correlation was observed between SCOD concentration and the *Calamus*-BC dosage ($R^2 = 0.9363$). This result could be ascribed to that *Calamus*-BC promoted the CH_4 production process and reduced the SCOD concentration, and these findings were consistent with the previous

Table 4 Kinetic parameters of methane production by the amended Gompertz equation

	Calamus-BC dosage (g/L)	λ (d)	R_{max} (L/kgVS/day)	P_0 (L/kgVS)	R^2	T_{90} (d)	T_{ef} (d)
BC0	0	0.61	13.80	177.31	0.9944	15.97	15.36
BC5	5	0.05	17.93	218.48	0.9904	14.62	14.57
BC10	10	0.00	19.95	221.86	0.9861	13.27	13.30
BC15	15	0.01	22.62	242.61	0.9924	12.83	12.82
BC20	20	0.19	24.30	233.13	0.9875	11.66	11.47

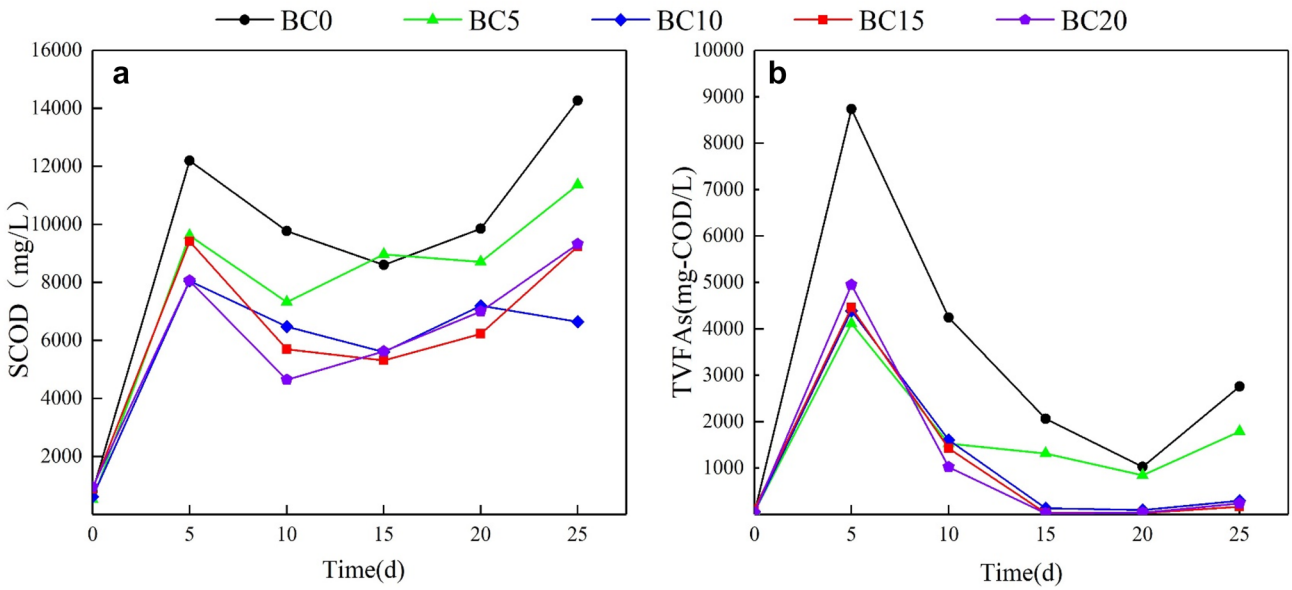

Fig. 3 Evolution of SCOD and TVFAs concentration in the liquid phase during TAD process: **a** SCOD; **b** TVFAs

results of the daily biogas production rate. In addition, the *Calamus*-BC reduced the SCOD concentration through adsorption due to its porous structure and large S_{BET}, as Siddique and Wahid [35] reported. Moreover, during days 10 to 20, the SCOD concentrations of BC10, BC15, and BC20 were significantly lower than those of BC0 and BC5, indicating that the adsorption and the degradation of SCOD were more evident when the *Calamus*-BC dosage reached a certain concentration.

As the important intermediates in TAD, the TVFA concentration represented the acidification stage of the sludge, which usually accounted for about 50% of the SCOD concentration [36]. Figure 3b shows that the TVFA concentration in the control group is higher than those of the *Calamus*-BC addition during the TAD process. The results showed that the substrate was difficult to digest without biochar and the addition of biochar could avoid acidification and improve the stability of TAD, which were consistent with the results of Shen et al. [37].

Figure 4 illustrates the evolution of different VFAs (i.e., acetate, propionate, butyrate, isobutyrate, valerate, and isovalerate) under different *Calamus*-BC dosages during TAD. The main components of VFAs were acetate, propionate, and isovalerate in the early stage of TAD (days 1–10) in all groups. However, the VFAs except for acetate and propionate were degraded almost completely after 20 days. Acetate is the main component of the VFAs and an important intermediate of the CH_4 production process. The peak concentrations of acetate negatively correlated with the dosage of *Calamus*-BC ($R^2 = 0.9747$), indicating that *Calamus*-BC promoted the degradation of acetate to produce CH_4. The propionate is the most difficult intermediate to be degraded in the AD process. On the 15th day of TAD, the concentrations of propionate were 1417.94 (BC0), 547.28 (BC5), 48.08 (BC10), 0.00 (BC15), and 15.0 (BC20) mg/L. It is worth noting that the contents of acetate and propionate in BC0 and BC5 were higher than those in other groups. These results indicated that the long-SRT sludge is difficult to be digested, but the addition of a certain amount of *Calamus*-BC (≥ 10 g/L) can promote substrate degradation in a relatively short time. Similarly, Watanabe et al. [38] found that the propionate accumulation in the control group was earlier than that in the test group with biochar, and Giwa et al. [39] also believed that biochar accelerated the degradation of acetate and propionate during AD.

The changes in butyrate, isobutyrate, valerate, and isovalerate (Fig. 4c–f) in the test groups with *Calamus*-BC addition were reduced and degraded completely at the end of the TAD. The concentrations of butyrate and isobutyrate in the test groups were low throughout the AD process and significantly different from those in the control group, indicating that *Calamus*-BC evidently promoted the degradation of butyrate (> 93.47%) and isobutyrate (> 75.47%).

Figure 5 shows the changes in pH, TAN, and FAN in the liquid phase during the TAD process. The pH is affected by many factors, such as temperature, alkalinity, VFAs, and NH_3 concentration [40]. After 5th days of AD, the pH value of each test group remained in the slightly alkaline range (8.10–8.40), which was significantly higher than that of the control group. because of the alkalinity of *Calamus*-BC. Wang et al. [32] reported that the alkalinity of biochar increased the pH of TAD systems by promoting the conversion of CO_2 to HCO_3^-, or CO_3^{2-}, reducing the VFA accumulation and improving the reactor stability.

Except for VFAs, TAN is another typical inhibitor to anaerobic digestion inhibitor, the inhibitory concentration of TAN ranges from 1500 to 7000 mg/L [41]. As shown in Fig. 5b, the change trends of TAN in all groups are similar. The final TAN concentrations were 2320.79 (BC0), 2309.79 (BC5), 2353.79 (BC10), 2548.28 (BC15), and 2430.78 (BC20) mg/L, indicating that the addition of *Calamus*-BC had no significant effect on TAN in TAD of the long-SRT sludge. Figure 5c shows the change trends of FAN concentration along the TAD process. The FAN concentrations in the test groups were significantly higher than those in the control group, which were 774.90 (BC0), 1022.60 (BC5), 936.52 (BC10), 1116.34 (BC15), and 1131.66 (BC20) mg/L at the end of the TAD, indicating that the decrease in the CH_4 production in BC20 might be caused by the FAN inhibition (Fig. 2). This result showed that the CH_4 production in TAD of sludge was inhibited by the accumulation of FAN especially the TAD with excess *Calamus*-BC.

Conclusion

Calamus-BC addition enhanced CH_4 production and yield through the increased conductivity and pH in TAD of long-SRT sludge. The optimal dosage was 15 g *Calamus*-BC/L, which increased which increased 43.4% of cumulative CH_4 production, while reduced 0.6 days of the lag phases compared with the control group. The control system was not capable of fully removing short VFA, which made WAS indigestible, but the addition of *Calamus*-BC effectively reduced the accumulation of VFA and promote DIET process in TAD. However, the synergistic reaction of long-SRT sludge and *Calamus*-BC addition might lead to a high FAN concentration, which may have a negative effect on the CH_4 production process. Hence, the appropriate dosage of *Calamus*-BC is crucial. This study showed that biochar made from wetland plants represented by *Calamus* can effectively promote the anaerobic digestion of sludge and achieve the purpose of treating waste with waste.

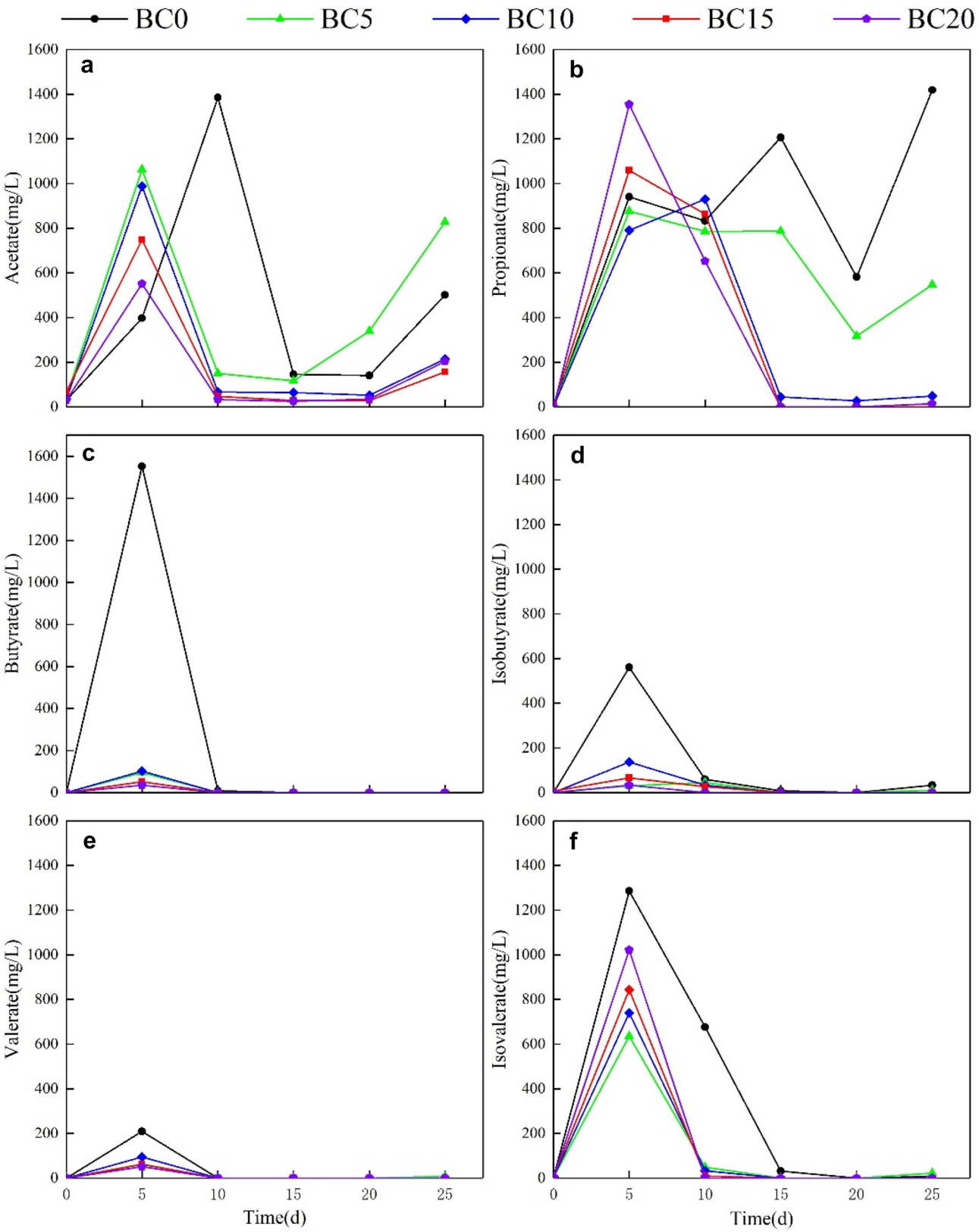

Fig. 4 Evolution of different VFAs in TAD: **a** acetate; **b** propionate; **c** butyrate; **d** isobutyrate; **e** valerate and **f** isovalerate concentration during TAD process

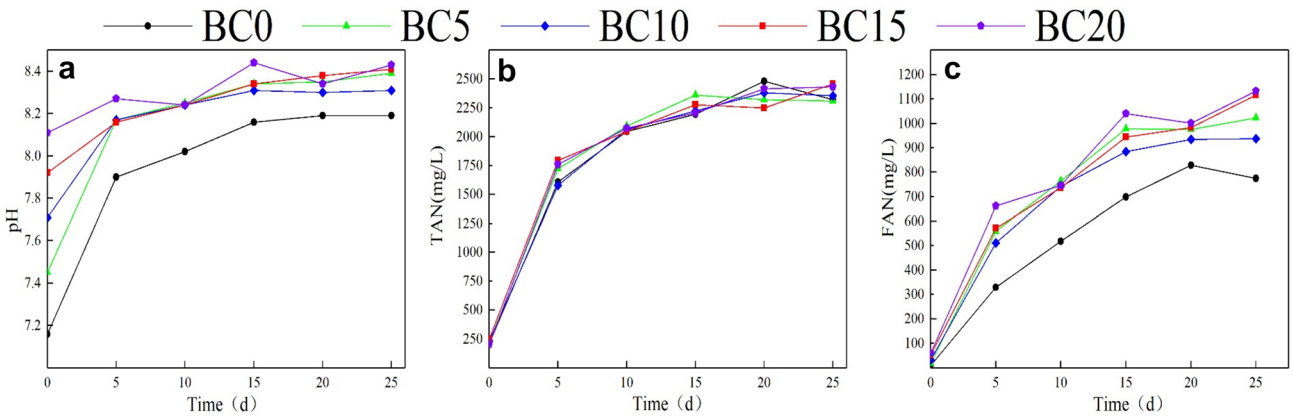

Fig. 5 Changes of pH, TAN and FAN concentration in the liquid phaseduring TAD process: **a** pH; **b** TAN; **c** FAN

Supplementary Information The online version contains supplementary material available at https://doi.org/10.1007/s12649-022-01693-1.

Acknowledgements This work was supported by the science and technology innovation demonstration project of social development of Xi'an Science and Technology Bureau (Grant Number: 20SFSF0011) and Key Research and Development Program of Shaanxi Province (2021ZDLSF05-04)

Data Availability Data for this study are available.

Declarations

Conflict of interest The authors declare that they have no conflict of interest.

References

1. Liu, H., Leng, F., Chen, P., Kueppers, S.: Pollutant removal characteristics of a two-influent-line BNR process performing denitrifying phosphorus removal: role of sludge recycling ratios. Water Sci. Technol. **74**(10), 2474–2482 (2016). (In Shanghai, China). https://doi.org/10.2166/wst.2016.438
2. Guang, Y., Guangming, Z., Hongchen, W.: Current state of sludge production, management, treatment and disposal in China. Water Res. **78**, 60–73 (2015). https://doi.org/10.1016/j.watres.2015.04.002
3. Atelge, M.R., Krisa, D., Kumar, G., Eskicioglu, C., Nguyen, D.D., Chang, S.W., Atabani, A.E., Al-Muhtaseb, A.H., Unalan, S.: Biogas production from organic waste: recent progress and perspectives. Waste Biomass Valoriz. **11**, 1019–1040 (2020). https://doi.org/10.1007/s12649-018-00546-0
4. Lafratta, M., Thorpe, R.B., Ouki, S.K., Shana, A., Germain, E., Willcocks, M., Jacquetta, L.: Demand-driven biogas production from anaerobic digestion of sewage sludge: application in demonstration scale. Waste Biomass Valoriz. **12**, 6767–6780 (2021). https://doi.org/10.1007/s12649-021-01452-8
5. Bi, S., Qiao, W., Xiong, L., Ricci, M., Adani, F., Dong, R.: Effects of organic loading rate on anaerobic digestion of chicken manure under mesophilic and thermophilic conditions. Renew. Energy. **139**, 242–250 (2019). https://doi.org/10.1016/j.renene.2019.02.083
6. Li, J., Hao, X., Loosdrecht, M.V., Luo, Y., Cao, D.: Effect of humic acids on batch anaerobic digestion of excess sludge. Water Res. **155**, 431–443 (2019). https://doi.org/10.1016/j.watres.2018.12.009
7. Junior, I.V., Almeida, R.D., Cammarota, M.C.: A review of sludge pretreatment methods and co-digestion to boost biogas production and energy self-sufficiency in wastewater treatment plants. J. Water Process. Eng. **40**, 101857 (2020). https://doi.org/10.1016/J.JWPE.2020.101857
8. Yang, L., Huang, Y., Zhao, M., Huang, Z., Miao, H., Xu, Z., Ruan, W.: Enhancing biogas generation performance from food wastes by high-solids thermophilic anaerobic digestion: effect of pH adjustment. Int. Biodeterior. Biodegrad. **105**, 153–159 (2015). https://doi.org/10.1016/j.ibiod.2015.09.005
9. Mao, C., Feng, Y., Wang, X., Pinjing, H.: Review on research achievements of biogas from anaerobic digestion. Renew. Sust. Energ. Rev. **45**, 540–555 (2015). https://doi.org/10.1016/j.rser.2015.02.032
10. Yeniguen, O., Demirel, B.: Ammonia inhibition in anaerobic digestion: a review. Process. Biochem. **48**(5–6), 901–911 (2013). https://doi.org/10.1016/j.procbio.2013.04.012
11. Beevi, B.S., Madhu, G., Sahoo, D.K.: Performance and kinetic study of semi-dry thermophilic anaerobic digestion of organic fraction of municipal solid waste. Waste Manage. **36**, 93–97 (2015). https://doi.org/10.1016/j.wasman.2014.09.024
12. Shi, J., Wang, Z., Stiverson, J.A., Zhongtang, Y., Yebo, L.: Reactor performance and microbial community dynamics during solid-state anaerobic digestion of corn stover at mesophilic and thermophilic conditions. Bioresour. Technol. **136**, 574–581 (2013). https://doi.org/10.1016/j.biortech.2013.02.073
13. Altinbas, M., Cicek, O.A.: Anaerobic co-digestion of chicken and cattle manures: free ammonia inhibition. Energy Sources **41**(7–12), 1097–1109 (2019). https://doi.org/10.1080/15567036.2018.1539143
14. Yang, Z., Wang, W., He, Y., Zhang, R., Liu, G.: Effect of ammonia on methane production, methanogenesis pathway, microbial community and reactor performance under mesophilic and thermophilic conditio-ns. Renew. Energy **125**, 915–925 (2018). https://doi.org/10.1016/j.renene.2018.03.032
15. Nakashimada, Y., Ohshima, Y., Minami, H., Yabu, H., Nishio, N.N.: Ammonia–methane two-stage anaerobic digestion of dehydrated waste-activated sludge. Appl. Microbiol. Biotechnol. **79**, 1061–1069 (2008). https://doi.org/10.1007/s00253-008-1501-7

16. Moestedt, J., Müller, B., Westerholm, M., Anna, S.: Ammonia threshold for inhibition of anaerobic digestion of thin stillage and the importance of organic loading rate. Microb. Biotechnol. **9**(2), 180–194 (2016). https://doi.org/10.1111/1751-7915.12330
17. Ryue, J., Lin, L., Kakar, F.L., Elbeshbishy, E., Al-Mamun, A., Dhar, B.R.: A critical review of conventional and emerging methods for improving process stability in thermophilic anaerobic digestion. Energy. Sustain. Dev. **54**, 72–84 (2020). https://doi.org/10.1016/j.esd.2019.11.001
18. Masahiko, M., Malvankar, N.S., Franks, A.E., Summers, Z.M., Lovley, D.R.: Potential for direct interspecies electron transfer in methanogenic wastewater digester aggregates. MBio **2**(4), e00159 (2011). https://doi.org/10.1128/mBio.00159-11
19. Zhao, Z., Zhang, Y., Yu, Q., Dang, Y., Li, Y., Quan, X.: Communities stimulated with ethanol to perform direct interspecies electron transfer for syntrophic metabolism of propionate and butyrate. Water Res. **102**, 475–484 (2016). https://doi.org/10.1016/j.watres.2016.07.005
20. Fagbohungbe, M.O., Herbert, B.M.J., Hurst, L., Ibeto, C.N., Semple, K.T.: The challenges of anaerobic digestion and the role of biochar in optimizing anaerobic digestion. Waste Manage. **61**, 236–249 (2017). https://doi.org/10.1016/j.wasman.2016.11.028
21. Lei, Y., Wei, L., Liu, T., Xiao, Y., Dang, Y., Sun, D., Holmes, D.E.: Magnetite enhances anaerobic digestion and methanogenesis of fresh leachate from a municipal solid waste incineration plant. Chem. Eng. J. **348**, 992–999 (2018). https://doi.org/10.1016/j.cej.2018.05.060
22. Zhao, Z., Zhang, Y., Li, Y., Dang, Y., Zhu, T., Quan, X.: Potentially shifting from interspecies hydrogen transfer to direct interspecies electron transfer for syntrophic metabolism to resist acidic impact with conductive carbon cloth. Chem. Eng. J. **313**, 10–18 (2017). https://doi.org/10.1016/j.cej.2016.11.149
23. González, J., Sánchez, M., Gómez, X.: Enhancing anaerobic digestion: the effect of carbon conductive materials. C J. Carbon Res. **4**(59), 1–19 (2018). https://doi.org/10.3390/c4040059
24. Fagbohungbe, M.O., Herbert, B.M.J., Hurst, L., Ibeto, C.N., Li, H., Usmani, S.Q., Semple, K.T.: The challenges of anaerobic digestion and the role of biochar in optimizing anaerobic digestion. Waste Manage. **61**, 236–249 (2017). https://doi.org/10.1016/j.wasman.2016.11.028
25. Xu, H., Chang, J., Wang, H., Liu, Y., Zhang, X., Liang, Y., Huang, X.: Enhancing direct interspecies electron transfer in syntrophic-methanogenic associations with (semi) conductive iron oxides: effects and mechanisms. Sci. Total Environ. **695**, 133876 (2019). https://doi.org/10.1016/j.scitotenv.2019.133876
26. Shen, Y., Linville, J.L., Leon, I.D., Schoene, R.P., Urgun-Demirtas, M.: Towards a sustainable paradigm of waste-to-energy process: enhanced anaerobic digestion of sludge with woody biochar. J. Clean. Prod. **135**, 1054–1064 (2016). https://doi.org/10.1016/j.jclepro.2016.06.144
27. Zhang, H., Tang, W., Wang, W., Yin, W., Zha, J.: A review on China's constructed wetlands in recent three decades: application and practice. J. Environ. Sci. **104**(6), 53–68 (2020). https://doi.org/10.1016/j.jes.2020.11.032
28. Andriamanohiarisoamanana, F.J., Saikawa, A., Tarukawa, K., Qi, G., Pan, Z., Yamashiro, T., Iwasaki, M., Ihara, I., Nishida, T., Umetsu, K.: Anaerobic co-digestion of dairy manure, meat and bone meal, and crude glycerol under mesophilic conditions: synergistic effect and kinetic studies. Energy Sustain. Dev. **40**, 11–18 (2017). https://doi.org/10.1016/j.esd.2017.05.008
29. Xiong, S., Deng, Y., Tang, R., Zhang, C., Zheng, J., Zhang, Y., Su, L., Yang, L., Liao, C., Gong, D.: Factors study for the removal of epoxiconazole in water by common biochars. Biochem. Eng. J. **161**, 107690 (2020). https://doi.org/10.1016/j.bej.2020.107690
30. Luo, C., Lü, F., Shao, L., He, P.: Application of eco-compatible biochar in anaerobic digestion to relieve acid stress and promote the selective colonization of functional microbes. Water Res. **68**, 710–718 (2015). https://doi.org/10.1016/j.watres.2014.10.052
31. Zhao, Z., Zhang, Y., Holmes, D.E., Dang, Y., Woodard, T.L., Nevin, K.P., Lovley, D.R.: Potential enhancement of direct interspecies electron transfer for syntrophic metabolism of propionate and butyrate with biochar in up-flow anaerobic sludge blanket reactors. Bioresour. Technol. **209**, 148–156 (2016). https://doi.org/10.1016/j.biortech.2016.03.005
32. Wang, G., Li, Q., Gao, X., Wang, X.: Sawdust-derived biochar much mitigates VFAs accumulation and improves microbial activities to enhance methane production in thermophilic anaerobic digestion. ACS Sustain. Chem. Eng. **7**, 2141–2150 (2018). https://doi.org/10.1021/acssuschemeng.8b04789
33. Shen, Y., Linville, J.L., Urgun-Demirtas, M., Schoene, R.P., Snyder, S.W.: Producing pipeline-quality biomethane via anaerobic digestion of sludge amended with corn stover biochar with in-situ CO_2 removal. Appl. Energy **158**, 300–309 (2015). https://doi.org/10.1016/j.apenergy.2015.08.016
34. Jang, H.M., Choi, Y.K., Kan, E.: Effects of dairy manure-derived biochar on psychrophilic, mesophilic and thermophilic anaerobic digestions of dairy manure. Bioresour. Technol. **250**, 927–931 (2017). https://doi.org/10.1016/j.biortech.2017.11.074
35. Siddique, M.N.I., Wahi, Z.A.: Achievements and perspectives of anaerobic co-digestion: a review. J. Clean. Prod. **194**, 359–371 (2018). https://doi.org/10.1016/j.jclepro.2018.05.155
36. Yu, L., Bian, C., Zhu, N., Shen, Y., Yuan, H.: Enhancement of methane production from anaerobic digestion of waste activated sludge with choline supplement. Energy **173**, 1021–1029 (2019). https://doi.org/10.1016/j.energy.2019.02.076
37. Shen, Y., Yu, Y., Zhang, Y., Urgun-Demirtas, M., Yuan, H., Zhu, N., Dai, X.: Role of redoxactive biochar with distinctive electrochemical properties to promote methane production in anaerobic digestion of waste activated sludge—ScienceDirect. J. Clean. Prod. **278**, 123212 (2021). https://doi.org/10.1016/j.jclepro.2020.123212
38. Watanabe, R., Tada, C., Baba, Y., Fukuda, Y., Nakai, Y.: Enhancing methane production during the anaerobic digestion of crude glycerol using Japanese cedar charcoal. Bioresour. Technol. **150**, 387–397 (2013). https://doi.org/10.1016/j.biortech.2013.10.030
39. Giwa, A.S., Xu, H., Chang, F., Wu, J., Li, Y., Ali, N., Ding, S., Wang, K.: Effect of biochar on reactor performance and methane generation during the anaerobic digestion of food waste treatment at long-run operations. J. Environ. Chem. Eng. **7**(4), 103067 (2019). https://doi.org/10.1016/j.jece.2019.103067
40. Ruffino, B., Campo, G., Cerutti, A., Zanetti, M., Lorenzi, E., Scibilia, G., Genon, G.: Preliminary technical and economic analysis of alkali and low temperature thermo-alkali pretreatments for the anaerobic digestion of waste activated sludge. Waste Biomass Valoriz. **7**(4), 667–675 (2016). https://doi.org/10.1007/s12649-016-9537-x
41. Han, B., Butterly, C., Zhang, W., He, J.Z., Chen, D.: Adsorbent materials for ammonium and ammonia removal: a review. J. Clean. Prod. **283**(12), 124611 (2020). https://doi.org/10.1016/j.jclepro.2020.124611

Authors and Affiliations

Yi Wang[1,2] · Zhi Wang[1,2] · Linping Wang[1,2] · Jun Peng[1,2] · Xiaomei Kou[3] · Lijuan Gao[3] · Shizhang Wu[3] · Baohua Chai[1,3] · Ke Zhao[1]

✉ Yi Wang
wangyi1003@sina.com; wangyi1003@xauat.edu.cn

[1] School of Environmental and Municipal Engineering, Xi'an University of Architecture and Technology, Xi'an, China

[2] Key Laboratory of Northwest Water Resource, Environment and Ecology, MOE, Xi'an University of Architecture and Technology, Xi'an 710055, People's Republic of China

[3] Power China-Northwest Engineering Corporation Limited, Xi'an 710065, China